A MICROSCOPIC ANALYSIS OF ELASTIC SCATTERING OF ^{8}Li NUCLEUS ON DIFFERENT TARGET NUCLEI

M. Aygun

Department of Physics, Bitlis Eren University, Bitlis, 13000, Turkey

(Received June 3, 2014; revised version received June 26, 2014)

We examine the elastic scattering angular distributions of ^{8}Li projectile by the different target nuclei from ^{9}Be to ^{208}Pb at various incident energies. In order to obtain a global potential set, we make the theoretical calculations for the same geometry of the reactions via the double folding model based on the optical model. We give the results as comparison with the experimental data.

DOI:10.5506/APhysPolB.45.1875
PACS numbers: 24.10.Ht, 25.60.Bx

1. Introduction

The technological developments provided in radioactive ion beam (RIM) facilities have opened new research areas in nuclear physics. Thus, the investigation of the radioactive nuclei such as ^{8}Li have been made possible. ^{8}Li is an interesting nucleus because of being neutron-rich nucleus and its role in astrophysics. ^{8}Li is generated in the radiative-capture reaction ^{7}Li(n, γ)^{8}Li known as inhomogeneous Big Bang [1]. ^{8}Li which has a separation energy at 2.033 MeV [2] decays to $^8\mathrm{Li} \to {^7\mathrm{Li}}+n$. For this reason, ^{8}Li nucleus has intensively been investigated and a great number of experimental data have been accumulated for the interaction with different target nuclei [3–13]. In these studies, the interactions have been analyzed by using different approaches. However, as far as we know, there is not a global optical model analysis via the double folding model of ^{8}Li nucleus scattered from light, medium and heavy mass target nuclei. Therefore, a global elastic scattering analysis of ^{8}Li by different target nuclei at various energies will be very interesting for determining general feature of interacting systems.

Alkhazov *et al.* [14] have given parameterizations of the nuclear density distributions of ^{4,6,8}He nuclei. Then, Dobrovolsky *et al.* [15] have reported the parameters obtained for ^{6,8,9,11}Li nuclei. In our study, we focus on the double folding model calculations based on the optical model by means of these parameterizations obtained for ^{8}Li. The optical model is a widely used model in explaining the elastic scattering angular distributions of the nucleus–nucleus interactions in nuclear physics. The optical model potential consists of two parts — real and imaginary. In order to obtain the real part of the potential, the double folding model together with the density distributions of both projectile nucleus and target nucleus [16] can be used. However, the imaginary potential can be assumed to be the Woods–Saxon potential. In the present study, we aim to investigate the elastic scattering angular distributions of ^{8}Li by different target nuclei from ^{9}Be to ^{208}Pb by using the double folding model. Then, we compare the results obtained with the experimental data. This comparison provides information about the validity of the model used in calculations.

In the next section, we present the theoretical model used in our calculations and the results of these calculations are presented in Section 3. Section 4 is devoted to our conclusions.

2. Theoretical analysis

We analysed the elastic scattering angular distributions of ^{8}Li+^{9}Be, ^{12}C, ^{27}Al, ^{58}Ni and ^{208}Pb systems via the double folding model based on the optical model. The $V_{\rm Nuclear}(r)$ potential has real and imaginary parts. To obtain the real part of the potential, the nuclear matter distributions of both projectile and target nuclei together with an effective nucleon–nucleon interaction potential (ν_{NN}) are used. Thus, the double folding potential is

$$V_{\rm Double\ Folding}(\boldsymbol{r}) = \int d\boldsymbol{r}_1 \int d\boldsymbol{r}_2 \rho_{\rm P}(\boldsymbol{r}_1)\rho_{\rm T}(\boldsymbol{r}_2)\nu_{NN}(\boldsymbol{r}_{12})\,, \tag{1}$$

where $\rho_{\rm P}(\boldsymbol{r}_1)$ and $\rho_{\rm T}(\boldsymbol{r}_2)$ are the nuclear matter density of projectile and target nuclei, respectively. In this context, we have used the Gaussian–Gaussian (GG) density distribution for ^{8}Li nucleus. We have assumed that ^{8}Li consists of the core (^{7}Li) and valence nucleon (n). Thus, the Gaussian density distribution for ^{7}Li and the Gaussian density distribution for n have been used. According to this, the ^{8}Li nuclear matter density is shown as following forms [14]

$$\rho_{\rm c}(r) = \left(\frac{3}{2\pi R_{\rm c}^2}\right)^{3/2} e^{\left(-\frac{3r^2}{2R_{\rm c}^2}\right)}\,, \tag{2}$$

$$\rho_{\rm v}(r) = \left(\frac{3}{2\pi R_{\rm v}^2}\right)^{3/2} e^{\left(-\frac{3r^2}{2R_{\rm v}^2}\right)}\,, \tag{3}$$

where R_c and R_v are the root mean square (rms) radii of the core and valence nucleon distributions, respectively. The total matter distribution ρ_m is given in the following form

$$\rho_m(r) = [N_c\rho_c(r) + (A - N_c)\rho_v(r)]/A\,, \tag{4}$$

where N_c and A are the number of nucleons in the core and the atomic number, respectively. The constant values for Eq. (2) and Eq. (3) have been taken from [15]. In Fig. 1, GG density distribution used for ^{8}Li are shown. We have chosen the Gaussian form for ^{12}C ground state matter density distribution

$$\rho(r_1) = \rho_0\ \left(1 + wr_1^2\right)\ \exp\ \left(-\beta r_1^2\right)\,, \tag{5}$$

where $\rho_0 = 0.1644$ fm^{-3}, $w = 0.4988$ fm^{-2}, and $\beta = 0.3741$ fm^{-2} [17, 18]. The density distributions of the other target nuclei have been taken from RIPL-3 [19].

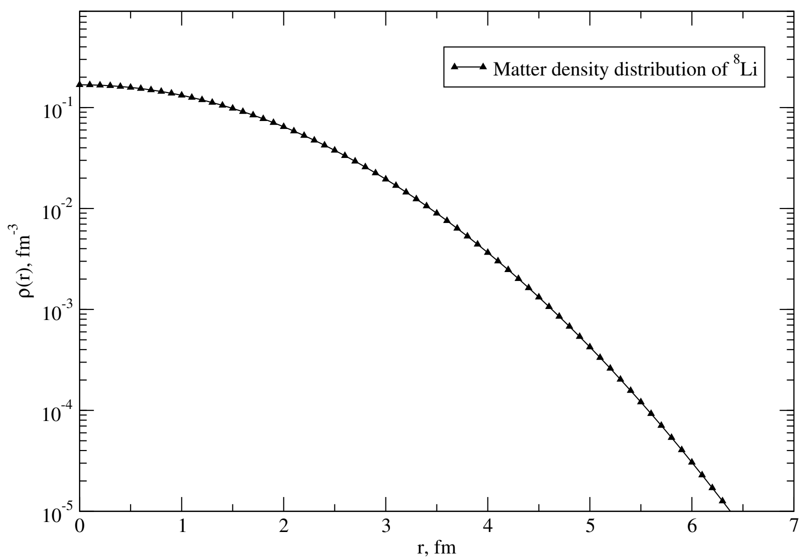

Fig. 1. The matter density distribution of ^{8}Li nucleus within the GG density distribution.

The effective nucleon–nucleon interaction, ν_{NN}, is integrated over both density distributions. Several nucleon–nucleon interaction expressions can be used for the folding model potentials. We have chosen the most common one, the M3Y nucleon–nucleon (Michigan 3 Yukawa) realistic interaction, which is given by [16]

$$\nu_{NN}(r) = 7999\,\frac{\exp(-4r)}{4r} - 2134\,\frac{\exp(-2.5r)}{2.5r} + J_{00}(E)\delta(r)\ \text{MeV}\,, \tag{6}$$

where $J_{00}(E)$ represents the exchange term, since nucleon exchange is possible between the projectile and the target. $J_{00}(E)$ has a linear energy-dependence and can be expressed as

$$J_{00}(E) = \ 276 \ [1 - 0.005 \ E_{\mathrm{Lab}}/A_p] \ \mathrm{MeV\ fm}^3 \,. \tag{7}$$

To obtain the imaginary part of the nuclear potential, Woods–Saxon type potential of the following form has been used

$$W(r) = -\frac{W_0}{1 + \exp\left((r - R_w)/a_w\right)} \,, \tag{8}$$

where $R_w = r_w \ (A_{\mathrm{P}}^{1/3} + A_{\mathrm{T}}^{1/3})$ and A_{P} and A_{T} are mass numbers of projectile and target nuclei respectively. The code FRESCO [20] has been used for the calculations. FRESCO is a general-purpose reaction code, with possibility to search for parameters of the optical model (via requirements to fit the data *e.g.* angular distributions).

3. Results and discussion

We have investigated the elastic scattering angular distribution of ^{8}Li projectile scattered from target nuclei including ^{9}Be, ^{12}C, ^{27}Al, ^{58}Ni and ^{208}Pb. When the real potential is obtained via the double folding model, we have used the GG density distribution for ^{8}Li. The imaginary potential has been taken as the Woods–Saxon potential. In order to obtain good agreement results with the experimental data, we have searched for the depth (W_0), the radius (r_w) and the diffusion parameter (a_w) of the imaginary potential. We have wanted to perform a global analysis for the same geometry of all the interactions and have kept the value of r_w fixed at 1.34 fm. Then, we have varied W_0 and a_w values in order to optimize the fit to the data. We have used $a_w = 0.90$ fm value for all the systems. At these values of r_w and a_w, W_0 values have been adjusted to obtain the agreement results with the experimental data for each system. The optical model parameters (imaginary part) are presented in Table I. The normalization constant (N_R) used in the double folding calculations shows the achievement of the model used in the theoretical calculations. The most suitable value of the N_R is 1.0. With this goal, in our calculations, we have not changed this value and have taken it as 1.0. In Figs. 2 and 3 we have shown the obtained results. The solid line shows the results of GG density distribution used in calculations. As seen from figures, our results are generally in agreement with the experimental data. However, our results miss some points of the data because of using the same geometry for all the system. Also, further data for some reactions such as ^{8}Li+^{27}Al and ^{8}Li+^{208}Pb are needed.

TABLE I

The optical model parameters, cross-sections and χ^2 values that determine the agreement between the experimental data and the theoretical calculations. The normalization constant is 1.0 and the Coulomb radius is 1.30 fm.

System —	E_{Lab} [MeV]	W [MeV]	r_w [fm]	a_w [fm]	σ [mb]	χ^2 —
^{8}Li + ^{9}Be	27	21.00	1.34	0.90	2103	16.03
^{8}Li + ^{12}C	14	10.76	1.34	0.90	1623	0.49
^{8}Li + ^{27}Al	14	3.66	1.34	0.90	1203	1.57
^{8}Li + ^{58}Ni	19.6	12.96	1.34	0.90	1445	0.45
^{8}Li + ^{208}Pb	34.35	12.36	1.34	0.90	1302	4.81

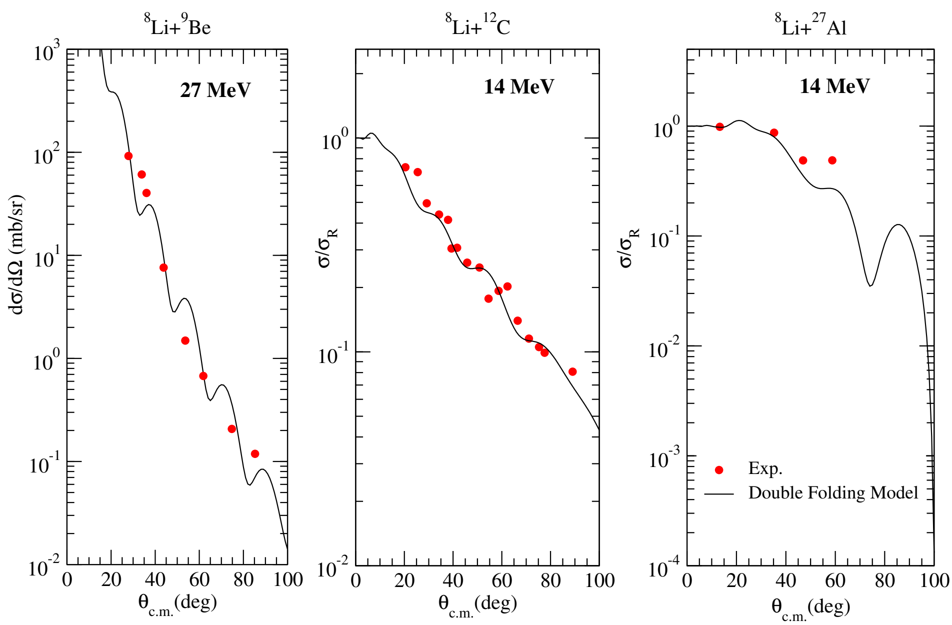

Fig. 2. Elastic scattering angular distributions for ^{8}Li+^{9}Be, ^{12}C, and ^{27}Al. The solid lines show the double folding model results, while the circles show the experimental data, which have been taken from [11, 12].

We have also calculated χ^2 values for all the reactions and have given the results in Table I. As seen from Table I, ^{8}Li+^{9}Be has the biggest χ^2 value and the smallest χ^2 value has been found for ^{8}Li+^{58}Ni reaction. The other χ^2 values are within a reasonable limit.

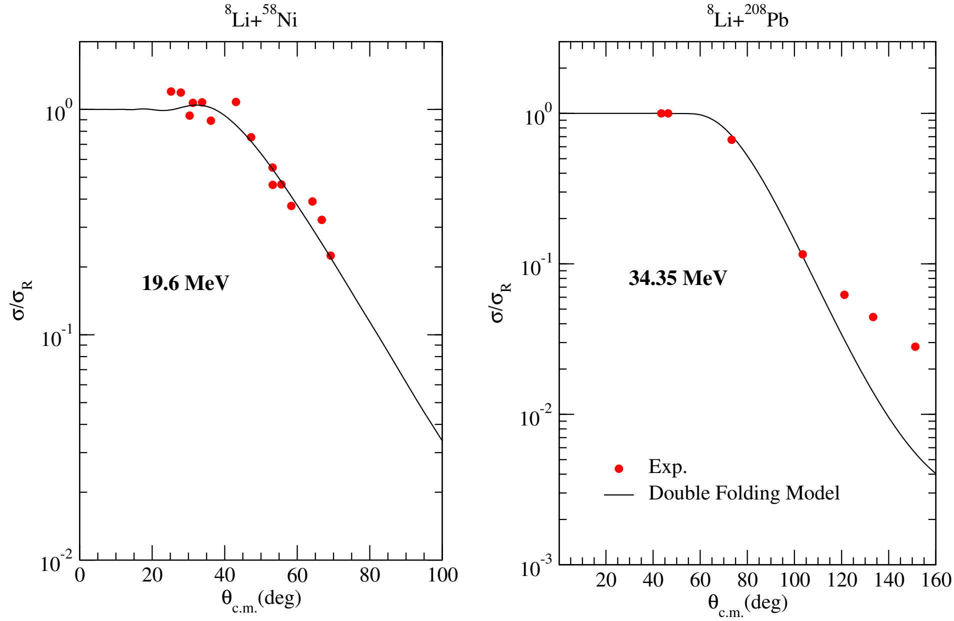

Fig. 3. Elastic scattering angular distributions for ^{8}Li+^{58}Ni, and ^{208}Pb. The solid lines show the double folding model results, while the circles show the experimental data, which have been taken from [11, 13].

In Table I, we have given the total reaction cross-sections for all the interactions at each energy. If one compares our results with the previous studies, one realizes that our results are close to the results of the literature [11]. According to this, while the difference for ^{8}Li+^{12}C is 260 mb, for ^{8}Li+^{27}Al is 99 mb or for ^{8}Li+^{58}Ni is 83 mb. Thus, it can be said that agreement between the results obtained for the different theoretical approaches is due to the interactions potentials used in the theoretical calculations being "phase equivalent" [21–23].

The shapes of the real and the imaginary potentials used in the elastic scattering calculations of ^{8}Li nucleus scattered from different target nuclei at various energies are shown in Fig. 4. It has been observed that the real potential of ^{8}Li+^{9}Be goes to zero faster than the other potentials and is shallower. As concerns imaginary potentials, one observes that ^{8}Li+^{9}Be potential is deeper than the other potentials.

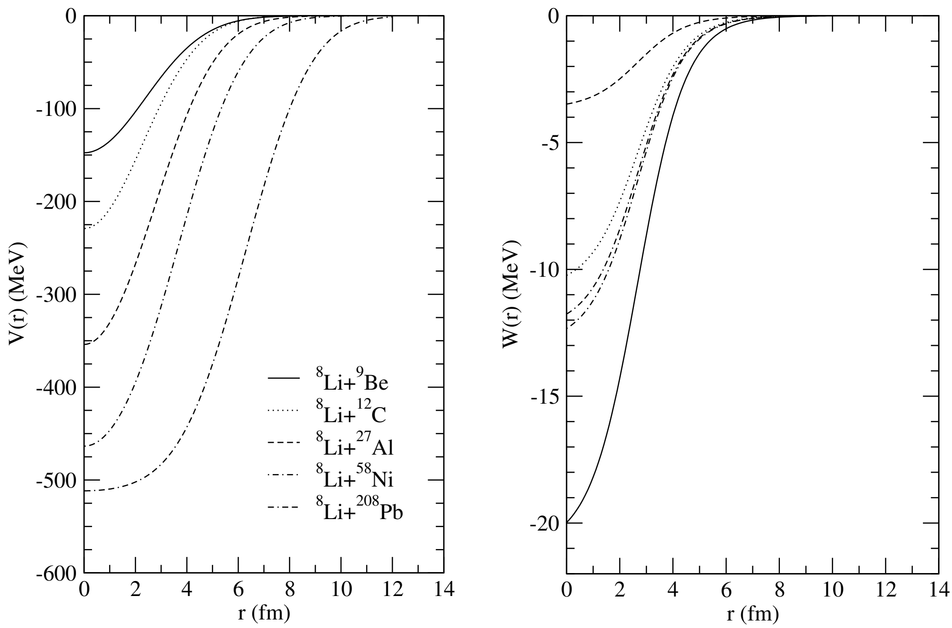

Fig. 4. The shapes of the real and the imaginary potentials of the nuclear potential of ^{8}Li which interacts with different target nuclei.

4. Conclusions

In this study, we have analyzed the elastic scattering angular distributions of ^{8}Li projectile by ^{9}Be, ^{12}C, ^{27}Al, ^{58}Ni and ^{208}Pb target nuclei at various energies. We have used the double folding model within the framework of the optical model and have given all the optical model parameters in Table I. We have shown the theoretical results in Figs. 2 and 3. The obtained cross-sections and χ^2 values are also shown in Table I. Finally, we have shown the real and the imaginary potentials of all the systems investigated in Fig. 4. We have seen that the folding model results are generally in agreement with the experimental data.

In summary, the article presents global analysis of the elastic scattering angular distributions of ^{8}Li interacting with different other nuclei. Double folding optical model approach has been used. As far as we know, there is not such a complementary study of elastic scattering for systems ^{8}Li-other nucleus by means of double folding model analysis.

Author thanks the Referee for valuable discussion and comments on the manuscript.

REFERENCES

[1] E.T. Ibraeva, M.A. Zhusupov, O. Imambekov, Sh.Sh. Sagindykov, *Phys. At. Nucl.* **71**, 1272 (2008).

[2] S. Mukherjee *et al.*, *Eur. Phys. J.* **A45**, 23 (2010).

[3] H. Yin-Lu, G. Hai-Rui, Z. Yue, Z. Jing-Shang, *Commun. Theor. Phys.* **50**, 463 (2008).

[4] O. Camargo *et al.*, *Phys. Rev.* **C78**, 034605 (2008).

[5] V. Guimarães, *Pramana — J. Phys.* **75**, 137 (2010).

[6] F.D. Becchetti *et al.*, *Phys. Rev.* **C71**, 054610 (2005).

[7] A. Lépine-Szily, R. Lichtenthäler, *Nucl. Phys.* **A787**, 94c (2007).

[8] A. Barioni *et al.*, *Phys. Rev.* **C80**, 034617 (2009).

[9] R.J. Smith *et al.*, *Phys. Rev.* **C43**, 5 (1991).

[10] P. Egelhof, *Nucl. Phys.* **A722**, 254c (2003).

[11] F.D. Becchetti *et al.*, *Phys. Rev.* **C48**, 308 (1993).

[12] V. Guimarães *et al.*, *Phys. Rev.* **C75**, 054602 (2007).

[13] J.J. Kolata *et al.*, *Phys. Rev.* **C65**, 054616 (2002).

[14] G.D. Alkhazov *et al.*, *Nucl. Phys.* **A712**, 269 (2002).

[15] A.V. Dobrovolsky *et al.*, *Nucl. Phys.* **A766**, 1 (2006).

[16] G.R. Satchler, W.G. Love, *Phys. Rep.* **55**, 183 (1979).

[17] M. El-AzabFarid, M.A. Hassanian, *Nucl. Phys.* **A678**, 39 (2000).

[18] M. Karakoc, I. Boztosun, *Phys. Rev.* **C73**, 047601 (2006).

[19] Reference Input Parameter Library (RIPL-3), `http://www-nds.iaea.org/RIPL-3/`

[20] I.J. Thompson, *Comput. Phys. Rep.* **7**, 167 (1988).

[21] B. Gonul, O. Ozer, M. Ylmaz, *Eur. Phys. J.* **A9**, 19 (2000).

[22] D. Baye, *Phys. Rev. Lett.* **58**, 2738 (1987); *J. Phys. A* **20**, 5529 (1987).

[23] M. Aygun, *G.U.J. Sci.* **27**, 2 (2014).